A simplified method for predicting the settlement of circular footings on multi-layered geocell-reinforced non-cohesive soils

S.N. Moghaddas Tafreshi [1], T. Shaghaghi[2], Gh. Tavakoli Mehrjardi[3], A.R. Dawson[4], M. Ghadrdan[5]

[1]*Corresponding Author, Department of Civil Engineering, K.N. Toosi University of Technology, Tehran, Iran. Tel: +982188779473; Fax: +982188779476; E-mail address: nas_moghaddas@kntu.ac.ir*

[2]*MSc graduated, Department of Civil Engineering, K.N. Toosi University of Technology, Tehran, Iran. Tel: +982188779473; Fax: +982188779476; E-mail address: tahereh.shaghaghi@gmail.com*

[3]*Department of Civil Engineering, Faculty of Engineering, University of Kharazmi, Tehran, Iran E-mail address: ghtavakoli@khu.ac.ir*

[4]*Nottingham Transportation Engineering Centre, University of Nottingham, Nottingham, UK. Tel: +441159513902; Fax: +441159513909; E-mail address: andrew.dawson@nottingham.ac.uk*

[5]*MSc graduated, Department of Civil Engineering, K.N. Toosi University of Technology, Tehran, Iran. Tel: +982188779473; Fax: +982188779476; E-mail address:mg1365@gmail.com*

Abstract: Multiple layers of geosynthetic reinforcement, placed below foundations or in the supporting layers of road pavements, can improve section performance through several mechanisms, leading to reduction in stresses and deformations. This paper aims to present a new analytical solution, based on the theory of multi-layered soil system to estimate the pressure-settlement response of a circular footing resting on such foundations, specifically those containing geocell layers. An analytical model that incorporates the elastic characteristics of soil and reinforcement is developed to predict strain and confining pressure propagated throughout an available multi-layer system, is proposed. A modified elastic method has been used to back-calculate the elastic modulus in terms of strain and confining pressure with materials data extracted from triaxial tests on unreinforced and geocell-reinforced soil samples. The proposed model has been validated by results of plate load tests on unreinforced and geocell-reinforced foundation beds. The comparisons between the results of the plate load tests and proposed analytical method reflected a satisfactory accuracy and consistency, especially at expected, practical, settlement ratios. Furthermore, to have a better assessment of geocell-reinforced foundations' behavior, a parametric sensitivity has been studied. The results of this study show that the higher bearing pressure and lower settlement were achieved when number of geocell layer, secant modulus of geocell and the modulus number of the soil were increased. These results are in-line with the experimental results of the previous researchers. The study also permits the limits of effective and efficient reinforcement to be determined.

1. Introduction

In the last decades, due to its cost savings, ease of construction and ability to improve the visual appearance, geosynthetic reinforced soil has been significantly exploited in geotechnical engineering applications such as road construction, railway embankments, lifeline provision, stabilization of slopes, and improvement of soft foundation beds (e.g., Collin et al., 1996; Raymond, 2002; Hufenus et al., 2006; Dash et al., 2007; Bathurst et al., 2009; Madhavi Latha and Somwanshi, 2009a; Zhang et al., 2009; Ling et al., 2009; Palmeira and Andrade, 2010; Pokharel et al., 2010; Boushehrian et al., 2011; Lambert et al., 2011; Yang et al. 2012; Thakur et al., 2012; Tavakoli Mehrjardi et al., 2012; Leshchinsky and Ling, 2013a,b; Yang and Han, 2013; Tanyu et al., 2013, Chen et al., 2013, Soudé et al., 2013; Avesani Neto et al., 2013; Kachi et al., 2013; Moghaddas Tafreshi et al., 2014; Indraratna et al., 2015). A desirable use of such reinforcements would be to improve the bearing capacity and settlement of footings. With this in mind, many researchers have investigated the beneficial ability of planar and cellular reinforcement (e.g. geocell) constructions and how best to arrange the inclusions so as to deliver effective reinforcement and to improve their bearing capacity and settlement response (Dash et al., 2007; Sitharam et al., 2007; Madhavi Latha and Rajagopal, 2007; Zhou and Wen, 2008; Chen and Chiu, 2008; Yoon et al., 2008; Sharma et al., 2009; Wesselo et al., 2009; Sireesh et al., 2009; Eid et al., 2009, Pokharel et al., 2010; Zhang et al., 2010a; Yang et al., 2012; Lambert et al., 2011; Kumar and Kaur, 2012; Tanyu et al., 2013; Tavakoli mehrjardi et al., 2013; Dash and Chandra Bora, 2013; Chen et al., 2013; Mehdipour et al., 2013; Biswas et al., 2013; Hegde and Sitharam, 2014; Huang, 2014, Song et al., 2014).

Recently, two of the current authors have shown that geocell reinforcement can be significantly more effective than a planar reinforcement, in improving the behaviour of foundation beds under static and repeated loads (Moghaddas Tafreshi and Dawson, 2010a;b). They attributed this to the superior confinement offered by the geocells in all directions, due to the frictional and passive resistance developed at the soil-geocell interfaces that increases the sand's bearing capacity and decreases the settlement of the foundation bed.

An analytical approach to the design of such footings and to explain their pressure-settlement behavior would be very useful. Although, there have been many experimental studies into the use of geocell reinforcement in civil engineering works, there are few analytical studies (e.g., Zhang et al. 2009; 2010a;b). Zhang et al. (2010a) presented a simple bearing capacity calculation method for a geocell-supported embankment on a soft subgrade based on the study of the reinforcement functions of a geocell layer beneath a road embankment. They indicated that their results were relatively close to the experimental results. Zhang et al. (2010b) idealized a geocell-reinforced mattress as a beam on a Winkler foundation in order to analyze its settlement response. Semi-analytic

Page 2 of 33

62 solutions were developed to assess the deformations of, and internal forces in, the foundation 'beam'. They

63 reported that the interface resistance, related to the horizontal deformation of the composite beam (i.e., geocell-

64 soil 'beam'), had a reduction effect on the embankment settlement.

2. Aim

66 A literature review, briefly reported above, indicated that there remains a lack of analytical study into the

67 behaviour of footings supported by a geocell-reinforced bed, particularly when that bed includes a multi-layered

68 geocell. Therefore, this article seeks to redress this omission by providing a relatively simple analytical method,

69 based on "n"-layered soil system theory (Hirai, 2008) and surface settlement of equivalent system (Vakili et al.,

70 2008), for the evaluation of the pressure-settlement response of both unreinforced and multi-layered geocell-

71 reinforced foundation beds. The results of this method have been compared with the results of plate load tests

72 (Moghaddas Tafreshi et al., 2013) to investigate its validity. In addition, the effects of various parameters such as

73 geocell and soil stiffness modulus, geocell layer height and diameter of plate load have been investigated so as to

74 understand mechanisms for improving the pressure-settlements behaviour of such footings. Note that, although,

75 the settlement-stress behavior of plate loading tests is not elastic, yet the aforementioned analytical method

76 simulated the behavior as a Multiple Linear Elastic (MLE) model (i.e., non-linear elastic) permitting calculation

77 of the elastic modulus of each layer, for each loading step.

3. Problem statement

79 Geosynthetic inclusions are most effective if used in the zone significantly stressed by the footing. Since, a

80 concentrated stress bowl occupies a zone equal to or twice the depth of the footing width/diameter (the "effective

81 depth" being approximately 1.2 – 2 m for a typical footing width/diameter), and the heights of commercially

82 produced geocells are usually less than 200 mm (available cell depths produced by two key manufacturers in

83 Europe and USA), a single thick layer of geocell beneath the footing is not possible for field construction. Even

84 if it were, such a thick geocell layer would likely make compaction of cell-fill extremely difficult (Thakur et al.,

85 2012; Moghaddas Tafreshi et al., 2014), consequently decreasing the performance of a thick single layer of

86 geocell. Hence, practically, if such a depth of soil needs to be reinforced by geocells, it necessitates designers to

87 use 3 to 4 layers of geocell with thickness ≤ 200 mm.

88 Hence, the use of several layers of geocell (say, three or four) each with a thickness ≤ 200mm and with

89 vertical spacing between successive layers of geocell is a practical alternative and could be a beneficial

90 means of reinforcing the soil beneath a footing. The schematic cross-section of the foundation bed containing

91 geocell-reinforcement layers with the thicknesses of h_g, and of the footing, is shown in Fig. 1. In this figure,

92 the first geocell layer is located at a depth of u beneath the footing and the next geocell layers are placed after

93 an unreinforced soil thickness of h_s. It should be noted that, although there are three probable mechanisms by

94 which geocell transfers stress through the depth of foundation bed ("lateral resistance effect", "vertical stress

95 dispersion effect" and "membrane effect"), this study tried to simulate all these factors by considering soil-

96 geocell layer as a composite material. Some simplification for a complicated problem like the current system

97 is inevitable. Here, the characteristics of the composite material have been defined according to the soil and

98 soil-geocell specimens in triaxial tests; and the simplifying assumptions made in the solution system mean

99 that the behavior of the geocell layers are considered to be uniform layers that only deform vertically. Since

100 the "n"-layered soil system theory by (Hirai, 2008) and surface settlement of equivalent system (Vakili et al.,

101 2008) were employed for the evaluation of the pressure-settlement response of multi-layered geocell-

102 reinforced foundation beds, a summary of these methods is presented in Sections 5 and 6.

103 **4. Pressure-settlement variation of footing on unreinforced bed**

104 For a semi-infinite soil medium of the elastic modulus E_n and Poisson's ratio v_n, subjected to uniform

105 pressure q on a circular footing with radius a, the immediate settlement at the depth z below the center of flexible

106 footing is written as Eq. (1) (Harr, 1966). Eq. (1) is valid for a flexible footing and should be multiplied by $\pi/4$

107 for a rigid footing.

$$w(z) = \frac{2aq(1-v_n^2)}{E_n}\left(\sqrt{1+\frac{z^2}{a^2}} - \frac{z}{a}\right)\left\{1 + \frac{z/a}{2(1-v_n)\sqrt{1+\frac{z^2}{a^2}}}\right\} \tag{1}$$

108 **5. N-Layered Soil System Theory (Hirai, 2008)**

109 Hirai (2008) developed the elastic relationships of multilayer soil stiffness modulus that have been investigated,

110 previously, by Palmer and Barber (1940) and Odemark (1949). Fig. 2 shows a multi-layered soil system

111 composed of n-layers of soil subjected to vertical loads q. As shown in Fig. 2, the present procedure uses the

112 elastic moduli, i.e. Young's modulus of E_m, Poisson's ratio of v_m and thickness of H_m for m^{th} layer in n-layers of

113 multi-layered soil system. Parameters D and D_f are diameter and embedment depth of a footing, respectively.

114 The n-layered soil system shown in Fig. 2 was transformed into an equivalent two-layered soil system illustrated

115 in Fig. 3a. The equivalent elastic modulus of E_H (Hirai and Kamei, 2003; 2004) for ($n-1$) layers in Fig. 3a (where

116 $H=H_1+H_2+H_3+\ldots + H_{n-1}$) was represented by:

Page 4 of 33

$$E_H = \left[\left\{ E_1 \frac{(1-v_n^2)}{(1-v_1^2)} \right\}^{\frac{1}{3}} \frac{H_1 - D_f}{H - D_f} + \sum_{j=2}^{n-1} \left\{ E_j \frac{(1-v_n^2)}{(1-v_j^2)} \right\}^{\frac{1}{3}} \frac{H_j}{H - D_f} \right]^3 \tag{2}$$

117 Next, the two-layered soil system in Fig. 3a was transformed into an equivalent single soil layer with elastic

118 modulus of E_n and Poisson's ratio of v_n, (the thickness of an equivalent single layer is $H = H_e + H_n$) as shown in Fig.

119 3b, using the equivalent thickness relations (3) and (4) (Hirai and Kamei, 2003; 2004; Hirai, 2008). For the case

120 where $E_H \geq E_n$:

$$H_e - D_f = \left(\frac{E_H}{E_n} \right)^{1/3} (H - D_f) \tag{3}$$

121 and for the case where $E_H \leq E_n$:

$$H_e - D_f = \left[0.75 + 0.25 \left(\frac{E_H}{E_n} \right)^{1/3} \right] (H - D_f) \tag{4}$$

122 Likewise, Fig. 4 shows an equivalent system of soil layers to that previously illustrated in Fig. 2, but now each

123 soil layer has an equivalent thickness of H_{ie} and uniform E and v values for every layer (=E_n and v_n). Thus the

124 system is reduced to a single layer system of thickness $H_{1e} + H_{2e} + H_{3e} + \ldots + H_{(n-1)e} + H_n$ and stiffness properties E_n

125 and v_n. The equivalent thickness of each individual layer is required so as to obtain the thinning and strain of each

126 layer of the multilayered system as described in Section 7.2. According to the Palmer and Barber method (1940)

127 for a two-layer system and to Odemark's method (1949) for a multi-layered soil system, Eqs. (5a) and (5b),

128 respectively, were derived by Hirai (2008) for estimating the equivalent thickness of each layer for the case

129 where $E_m \geq E_n$:

$$H_{1e} - D_f = \left\{ \frac{E_1(1-v_n^2)}{E_n(1-v_1^2)} \right\}^{1/3} (H_1 - D_f) \tag{5a}$$

$$H_{me} = \left\{ \frac{E_m(1-v_n^2)}{E_n(1-v_m^2)} \right\}^{1/3} H_m \quad (m = 2 \sim n) \tag{5b}$$

130

131   For the case where $E_m \leq E_n$, by considering Terzaghi's approximate formula (1943), the equivalent thickness is

132   given by Eqs. (6a) and (6b):

$$H_{1e} - D_f = \left[0.75 + 0.25 \left\{ \frac{E_1(1-v_n^2)}{E_n(1-v_1^2)} \right\}^{1/3} \right] (H_1 - D_f) \tag{6a}$$

$$H_{me} = \left[0.75 + 0.25 \left\{ \frac{E_m(1-v_n^2)}{E_n(1-v_m^2)} \right\}^{1/3} \right] H_m \quad (m = 2 \sim n) \tag{6b}$$

133   where H_{1e} and H_{me} are the values of H_e for the first and subsequent layers ($m=2$ to n), respectively and E_1, v_1,

134   E_n, v_n and E_m, v_m are values of E_H and v for layers 1, n and $m=2$ to n, respectively.

135   **6. Surface Settlement of Equivalent System (Vakili et al., 2008)**

136   Vakili et al. (2008) developed the method of Foster and Ahlvin (1959) to evaluate the surface settlement of the

137   equivalent system shown in Fig. 4. According to this method, the actual vertical surface deflection of a footing

138   (w) was obtained by adding the amount of thinning, w_2, of the equivalent layer (with thickness of H_e) between

139   the surface ($z=0$) and a depth of $z=H_e$ to the vertical deflection at a depth of $z=H_e$ of a semi-infinite mass below

140   that depth (i.e. deflection of w_1 at bottom of the equivalent layer). In the case of uniform pressure "q" on a

141   flexible circular footing with radius "a" (Fig. 4), supported by a semi-infinite mass, w_1 is obtained by substituting

142   the value of $z=H_e$ from Eq. (3)/ or Eq. (4) into Eq. (1) to obtain Eq. (7):

$$w_1 = \frac{2aq(1-v_n^2)}{E_n} \left(\sqrt{1 + \left(\frac{H_e}{a}\right)^2} - \frac{H_e}{a} \right) \left(1 + \frac{H_e}{2a(1-v_n)\sqrt{1 + \left(\frac{H_e}{a}\right)^2}} \right) \tag{7}$$

143   Similarly, the vertical deflection at the center of loading on surface (i.e. w_0 at depth of $z=0$) of uniform equivalent

144   layer (i.e. for the footing on the equivalent layer), substituting the value of $z=0$ into Eq. (1) results:

$$w_0 = \frac{2a(1-v_n^2)q}{E_n} \tag{8}$$

145   Eqs. (7) and (8) are valid for a flexible footing and should be multiplied by $\pi/4$ for a rigid footing. The

146   vertical thinning of the equivalent layer (with thickness of H_e as in Fig 3b) between the loading surface ($z=0$) and

147   a depth of $z=H_e$ (i.e. (w_0-w_1)), can be converted to the thinning, w_2, of the original layer (thickness H as in Figs. 2

148   and 3a), using Eq. (9):

$$w_2 = \frac{E_n}{E_H}\left(w_0 - w_1\right) \tag{9}$$

149   Hence, Eqs. (7) and (9) may be summed to obtain the actual total surface settlement of the circular footing

150   ($w=w_1+w_2$).

151   **7. Pressure-settlement variation of footing on multi-layer geocell-reinforced bed**

152   **7.1. Methodology**

153   Fig. 5 shows a schematic model of a shallow circular footing with diameter, $D=2a$, located on a typical n-

154   layer foundation bed composed of "m" geocell layers and "n-m" soil layers, under the application of a

155   uniformly distributed surface load, q. The thicknesses of geocell and soil layers are h_g and h_s, respectively.

156   The first geocell layer is placed at a depth of u beneath the footing and the remaining geocell layers are

157   located after an unreinforced soil thickness of h_s. The effective depth, H_{eff}, is assumed as the depth to a point

158   below the footing at which only 10% of the applied stress on footing surface acts. The elastic modulus, E_i,

159   and Poisson's ratio, v_i ($i=1, 2, 3, ..., n$) of each layer is as given in Fig. 5. H_{n-1} is the thickness of the $(n-1)^{th}$

160   layer which can be calculated using Eq. (10).

$$H_{n-1} = H_{eff} - u - mh_g - (m-1)h_s \tag{10}$$

161   The following simplifying assumptions are made in this analysis, as follows:

162   • The soil layers are homogeneous, isotropic and non-cohesive;

163   • The unreinforced and reinforced layers deform only in the vertical direction;

164   • The footing is circular with no embedment depth, $D_f=0$;

165   • The behaviour of unreinforced and reinforced layers is assumed to be nonlinear elastic;

166   • Poisson's Ratio is assumed to be in the range 0.2 - 0.3 (see below).

167 Note that, although 'toothpaste' lateral squeezing of soil between geosynthetically-reinforced soil layers is a

168 possibility for plastic soils, granular soils are unlikely to experience this if the reinforcing layers confine the

169 granular soil closely. As observed in the tests at near full-scale by Wu et al. (2013), it is then the

170 reinforcement with the granular soil that controls, partly horizontal movement due to the frictional resistance

171 developed between the reinforcement and the soil and due to the nearby position of the reinforcing layers

172 disrupting potential shear planes/dislocation zones.

173 However, it is known that geocell layers don't expand much horizontally once properly filled with granular

174 soil and compacted (Dash et al., 2007; Pokharel, 2010). Thus the proposed analytical model does not directly

175 consider lateral deformation but, instead, allows for some, indirectly, by using:

176 (1) elasticity moduli of the soil and geocell-reinforced layers that were obtained from calibration of the

177 proposed equations (see Section 8.1) to the data obtained in the triaxial test that included some lateral

178 deformation, and

179 2) Poisson's Ratio values of 0.2 – 0.3, for the unreinforced and geocell-reinforced layers of the

180 foundation bed to compute the equivalent thickness of the multi-layered system (see Section 5), being in-line

181 with typical values as used by Mhaiskar and Mandal (1996) and Zhang et al. (2010c), as described later (see

182 Section 8.1.2).

183 **7.2. Incremental Formulation using Nonlinear Elastic Method**

184 As mentioned in section 2, the "n"-layered soil system theory (Hirai, 2008) and surface settlement of

185 equivalent system (Vakili et al., 2008) were employed to evaluate the pressure-settlement of footings

186 supported by a multi-layer geocell-reinforced bed as shown in Fig. 5. Fig. 3 shows the process of substituting

187 the n-layer system with an equivalent single-layer system, here with the limitation that D_f=0. To do so, firstly,

188 the upper "n-1" layers of thicknesses H_1, H_2, H_3, ….and H_{n-1} (Fig. 5) should be replaced by a single layer of

189 thickness (H_{eff}=H_1+H_2+H_3+….+ H_{n-1}) having an equivalent modulus of E_H in Fig. 6a (Hirai, 2008). The

190 equivalent elastic modulus (E_H) of layers 1 to n-1, is calculated by using Eq. (2) for the footing with no

191 embedment depth (D_f=0) as Eq. (11).

$$E_H = \left[\sum_{j=1}^{n-1} \left\{ E_i \frac{(1-v_n^2)}{(1-v_j^2)} \right\}^{\frac{1}{3}} \frac{H_j}{H_{eff.}} \right]^3 \tag{11}$$

192   where, H_i and E_i are the thickness and elastic modulus of ith layer, respectively. The n-layer system in Fig. 5

193   is thus reduced to a two layers system as shown in Fig. 6a.

194   The two-layered system (Fig. 6a) can be reduced to an equivalent single-layer system (Fig. 6b) with elastic

195   modulus of E_n and an equivalent thickness of H_e. The equivalent thickness (H_e) with the elastic modulus of E_n

196   and Poisson's Ratio of v_n is then defined by Eq. (12a) for the case where $E_H \geq E_n$ and by Eq. (12b) for the case

197   where $E_H \leq E_n$. Eq. (12a) and Eq. (12b) provided for the same Poisson's Ratio of the two layers in Fig. 6a

198   where E_n is the elastic modulus of the nth layer.

$$H_e = \left(\frac{E_H}{E_n} \right)^{1/3} H_{eff} \tag{12a}$$

$$H_e = \left[0.75 + 0.25 \left(\frac{E_H}{E_n} \right)^{1/3} \right] H_{eff} \tag{12b}$$

199   Consequently, the use of Eq. (11) and Eq. (12) deliver an equivalent single homogeneous semi-infinite mass

200   of material which can be substituted for the n-layer system as shown in Fig. 6b.

201   Generally, the footing settlement (i.e, soil surface settlement), w should be calculated using Eqs. (7) to

202   (10). Since, the nature of footing pressure-settlement variation is nonlinear, the behavior of unreinforced

203   layers and reinforced layers (Geocell and soil inside of its pockets) are considered to act as MLE (Multiple

204   Linear Elastic) layers. The MLE model provides an ability to calculate the elastic modulus of each layer, for

205   each load step, using the confining pressure of the current and previous stages as described in Eqs. (13) to

206   (23).

207   To calculate the elastic modulus of the ith layer, requires knowledge of the strain of layers 1 to n-1. To

208   compute these, the deformation and equivalent thickness of the ith layer (Fig. 5) are required. Using Eq. (5)

209   and Eq. (6) for the footing with no embedment depth (D_f=0), supported on a multi-layer system, the

210   equivalent thickness of each soil layer, H_{ie} with the same E_n and v_n was determined by Eq. (13a) for the case

211   where $E_i \geq E_n$ and by Eq. (13b) for the case where $E_i \leq E_n$, respectively.

$$H_{ie} = \left\{ \frac{E_i(1-v_n^2)}{E_n(1-v_i^2)} \right\}^{1/3} H_i \tag{13a}$$

$$H_{ie} = \left[0.75 + 0.25 \left\{ \frac{E_i(1-v_n^2)}{E_n(1-v_i^2)} \right\}^{1/3} \right] H_i \tag{13b}$$

212   Then, from Eqs. (7) and (9), for a rigid circular footing with radius a subjected to uniform pressure q, the

213   thinning and strain of the ith layer are defined as Eqs. (14) to (16):

$$w_i = \frac{2\pi a q(1-v_n^2)}{4E_n} \left(\sqrt{1 + \left(\frac{\sum_{l=1}^{l=i} H_{le}}{a}\right)^2} - \frac{\sum_{l=1}^{l=i} H_{le}}{a} \right) \left(1 + \frac{\sum_{l=1}^{l=i} H_{le}}{2a(1-v_n)\sqrt{1 + \left(\frac{\sum_{l=1}^{l=i} H_{le}}{a}\right)^2}} \right) \tag{14}$$

$$w_{p_i} = \frac{E_n}{E_i}\left(w_i - w_{i-1}\right) \tag{15}$$

$$\varepsilon_i = \frac{w_{p_i}}{H_i} \tag{16}$$

214   Where:

215   H_{ie}: equivalent thickness of the ith layer based on the elastic parameters of the nth layer

216   w_i: displacement at a depth of $\sum_{l=1}^{l=i} H_{le}$

217   w_{pi}: the vertical deformation within the ith layer of thickness H_{ie},(due to actual thinning of the ith layer)

218   ε_i: the strain across the thickness of the ith layer

219   In the jth loading step, the displacement increment of soil surface due to loading increment of q_j-q_{j-1} can be

220   calculated by Eqs. (17) to (20):

$$\Delta w_1^{\ j} = \frac{2\pi a(q_j - q_{j-1})(1-\upsilon_n^2)}{4E_n}(\sqrt{1+(\frac{H_e}{a})^2} - \frac{H_e}{a})(1+\frac{H_e}{2a(1-\upsilon_n)\sqrt{1+(\frac{H_e}{a})^2}}) \tag{17}$$

$$\Delta w_0^{\ j} = \frac{2\pi a(1-\upsilon_n^2)(q_j - q_{j-1})}{4E_n} \tag{18}$$

$$\Delta w_2^{\ j} = \frac{E_n}{E_H}\left(\Delta w_0^{\ j} - \Delta w_1^{\ j}\right) \tag{19}$$

$$w^{\ j} = w^{\ j-1} + \Delta w_1^{\ j} + \Delta w_2^{\ j} \tag{20}$$

221   Where:

222   $\Delta w_1^{\ j}$: vertical displacement increment on loading centerline at a depth of H_e for loading increment of q_j-q_{j-1}, (i.e.

223   at the bottom of the equivalenced layer)

224   $\Delta w_0^{\ j}$: vertical displacement increment at surface (of equivalent layer) beneath centre of load for loading

225   increment of q_j-q_{j-1},

226   $\Delta w_2^{\ j}$: vertical deformation (thinning) increment of the original layer of thickness of H,

227   $w^{\ j}$: vertical displacement at surface of system for loading of q_j.

228   Similarly, the strain increment for the ith layer at the jth loading step can be calculated using Eqs. (21) to (23)

229   using the adjustments already employed to formulate Eqs. (14) and (16):

$$\Delta w_i^{\ j} = \frac{2\pi a(q_j - q_{j-1})(1-\upsilon_n^2)}{4E_n}(\sqrt{1+(\frac{\sum_{l=1}^{l=i}H_{le}}{a})^2} - \frac{\sum_{l=1}^{l=i}H_{le}}{a})$$
$$(1+\frac{\sum_{l=1}^{l=i}H_{le}}{2a(1-\upsilon_n)\sqrt{1+(\frac{\sum_{l=1}^{l=i}H_{le}}{a})^2}}) \tag{21}$$

$$(\Delta w_p)_i^{\ j} = \frac{E_n}{E_i}\left(\Delta w_i^{\ j} - \Delta w_{i-1}^{\ j}\right) \tag{22}$$

$$\varepsilon_i^j = \varepsilon_i^{j-1} + \frac{(\Delta w_p)_i^j}{H_i} \qquad (23)$$

230   where:

231   H_{ie}: equivalent thickness of the ith layer based on the elastic parameters and thickness of the nth layer as defined
232   by Eq (13),

233   Δw_i^j : displacement increment of equivalent layer for layers 1 to i based on the elastic parameters of nth layer in

234   depth of $\sum\limits_{l=1}^{l=i} H_{le}$ for loading increment of q_j-q_{j-1},

235      $(\Delta w_p)_i^j$: deformation increment (thinning) of layer with thickness of H_i for loading increment q_j-q_{j-1},

236   ε_i^j : strain of layer with thickness of H_i subjected to loading q_j.

237   **8. Results and discussion**

238   To validate the results of the method presented above, the pressure-settlement response of a footing on

239   unreinforced and geocell-reinforced beds was estimated and compared with the results of four static plate

240   load tests (Moghaddas Tafreshi et al., 2013). As Fig. 7 shows, they performed the static plate load tests of a

241   footing supported on unreinforced soil and reinforced soil with geocell layers in a test pit measuring

242   2000×2000 mm in plane and 700 mm in depth using a 300 mm diameter rigid plate. The vertical distances of

243   the first layer of geocell (u) from the footing and also that from each other (h_s) were 0.2 times the footing

244   diameter. Also, the width of the geocell layers (b) was held constant at 5 times the footing diameter ($b/D=5$).

245   Since the horizontal dimensions of the test pit were about seven times bigger than the diameter of the footing

246   model and it was observed that the soil surface bulging around the footing model extended less than 1.5 times

247   the footing diameter from the circumference of the footing, the boundary effect of the pit walls on the test

248   results was likely insignificant. Also, regarding the test pit depth, the zone of influence of the footing will be

249   over a depth of less than 2 diameters beneath the footing (the "effective depth"), so the boundary effect of

250   test pit base on the test results may also be considered to be insignificant. Thus it should be viable to compare

251   the analysis results with the experimental ones.

252   The soil was well graded sand (SW, according to the Unified Soil Classification System, ASTM D 2487-

253   11) with a specific gravity of 2.68 and passing through the 38 mm sieve. The geocell used in the tests was

254   non-perforated and fabricated from continuous polypropylene filaments as a non-woven geotextile, with

255 ultimate tensile strength of 13.1 kN/m and pocket size of $110\times110\times100$ mm³ (lenght×width×height). The

256 details of engineering properties of the geotextile and soil properties are given by Moghaddas Tafreshi et al.,

257 (2013).

258 As part of this validation, the effects of several parameters including geocell and soil stiffness modulus,

259 geocell layer height and number of geocell layers on pressure-settlement response of footing were

260 investigated. The results of triaxial tests on unreinforced and geocell reinforced soil samples were used to

261 estimate the elastic modulus of the different layers during the loading steps (Noori, 2012). The soil, geocell

262 material and the density of the soil filled into the geocell pockets, used in both the plate load tests and triaxial

263 tests were the same. Six triaxial tests on unreinforced and reinforced soil samples with one layer of geocell, at

264 three confining pressures of 50, 100 and 150 kPa were conducted. The triaxial samples had a diameter of 100

265 mm and a height of 200 mm as shown in Fig. 8. The geocell-soil composites layers are of 100 mm in

266 diameter and 100 mm in height and positioned at mid-height of the specimen. The stress-strain response of

267 unreinforced and geocell reinforced samples with single layer of the geocel-soil composite under three

268 confining pressures are shown in Fig. 9. This figure indicates that the geocell reinforcement increases the

269 deviator stress (i.e., shear strength) of the samples considerably compared to unreinforced samples,

270 irrespective of confining pressure. This behavior is essentially due to the increase in confining effect of

271 geocell layers which cause an internal confinement in reinforced samples. On the other hand, vertical stress

272 applied to the infill induces a horizontal active pressure at the perimeter of the cell of geocell. The infill wall

273 interface friction transfers load into the cell structure which, in turn, mobilises resistance in surrounding cells.

274 It is also evident that cells that surround a loaded cell offer greater passive resistance due to the lateral strain

275 in the vicinity of the load– consequently leading to an improvement in the overall performance in strength.

276 Note that, triaxial compression tests on a single geocell layer sandwiched between two soil layers may give

277 different results compared to the test on a single, less constrained geocell. Since, the present analytical

278 formulation was employed to simulate the results of plate load tests supported by geocell layers of 100 mm

279 thickness, thus using a single layer of geocell with the same thickness in triaxial test sample with a height of

280 200 mm was inevitable.

281 **8.1. Elastic modulus of unreinforced and geocell-reinforced layers**

282 Since the six triaxial tests were conducted at three specified confining pressures of 50, 100 and 150 kPa, thus

283 the tangential elastic modulus at different strain levels can be obtained from the stress-strain responses in Fig. 9,

284   when the confining pressures are exactly 50, 100, and 150 kPa. Hence, at each stage of loading during the

285   analysis, a continuous function of confining pressure and axial strain is required to obtain the tangential elastic

286   modulus when the strain level and confining pressure being varied. Thus, in this section the elastic modulus of

287   unreinforced and geocell-reinforced soil layers in terms of strain and confining pressure, $E=f(\sigma_3,\varepsilon)$ for each

288   loading step, was modeled non-linearly from the data of six triaxial tests at the three confining pressures of 50,

289   100 and 150 kPa (see Fig. 9).

290   **8.1.1. Elastic modulus of unreinforced layers**

291   Based on the data extracted from Fig. 9a, the vertical stress ($\sigma_1=\sigma_3+\sigma_d$) of triaxial samples was found to be a

292   function of the confining pressure (σ_3) and axial strain (ε). Therefore a nonlinear regression model was

293   developed to estimate the vertical stress (σ_1) for different values of σ_3 and ε.

294   Several alternative modeling approaches were trialed before selecting, as optima, a non-linear power model

295   with of the largest multiple coefficient of determination, $R^2=0.91$, and a minimum value of standard error,

296     $E_s=0.11$, to estimate the vertical stress (σ_1) as a function of different parameters was obtained as Eq. (24):

$$\sigma_1 = 61.47\ \sigma_3^{0.73}\ \varepsilon^{0.34}\ e^{-3.17\varepsilon} \tag{24}$$

297   Using Eq. (24), the absolute average percentage of error, e_{ave} and maximum percentage of error, e_{max} in

298   estimating the value of σ_1 were found to be 2.5% and 4.6% respectively.

299   The tangential modulus of elasticity can be derived as the derivative of stress with respect to strain (from Eq.

300   (24)) as presented in Eq. (25a). The function of $f(\varepsilon)$ is defined in Eq. (25b).

$$E = 61.47\ \sigma_3^{0.73}*f(\varepsilon) \tag{25a}$$

$$f(\varepsilon) = (-3.17\ e^{-3.17\varepsilon}\varepsilon^{0.34} + \frac{0.34\ \varepsilon^{0.34}}{\varepsilon}e^{-3.17\varepsilon}) \tag{25b}$$

301   **8.1.2. Elastic modulus of geocell-reinforced layers**

302   Madhavi Latha (2000), based on the results of triaxial compression tests on geocell-encased sand, proposed

303   an empirical equation in the form of Eq. (26) to express the elastic modulus of the geocell reinforced sand (E_g).

$$E_g = 4\ \sigma_3^{0.7}(K_u\ +200M^{0.16}) \tag{26}$$

304   Where:

K_u: the dimensionless modulus number of the unreinforced sand in the hyperbolic model proposed by Duncan and Chang (1970),

M: the secant tensile modulus of the geocell material (e.g., geotextile and geogrid) in *kN/m,* assessed at an average strain of 2.5% in load-elongation, and

σ_3: the confining pressure in kPa.

In fact, the geocell layers are modeled as equivalent composite layers with enhanced stiffness and shear strength properties. The term in parentheses of Eq. (26) expresses the Young's modulus parameter of geocell-reinforced soil in terms of the secant modulus of the geocell material (M) and the dimensionless modulus number of the unreinforced soil (K_u).

However, due to the fact that the suggested relationship by Madhavi Latha (2000), Eq. (26), is not a function of axial strain level, it is modified to Eq. (27) as a function of both confining pressure (σ_3) and axial strain (ε).

$$E_g = a_1 \, \sigma_3^{b_1} (K_u + a_2 M^{b_2}) * f(\varepsilon) \tag{27}$$

The function of $f(\varepsilon)$ is assumed as Eq. (25b) and then the parameters of a_1, a_2, b_1 and b_2 are obtained from the triaxial tests results of geocell-reinforced soil (Fig. 9b).The constants parameters in Eq. (27) depend on the type of infill soil and strength of geocell material, which must be calibrated according to the results of triaxial tests on soil and geocell, with the same properties that would be used in the foundation bed. Fitting Eq. (27) to the data of Noori (2012) yields the elastic modulus as a function of σ_3, ε, K_u and M as Eq. (28).

$$E_g = 0.12 \, \sigma_3^{0.73} (K_u + 100 M^{0.1}) * f(\varepsilon) \tag{28}$$

At each loading step, the elastic modulus of unreinforced and reinforced layers were estimated using the confining pressure (at mid-height of the layer) and the strain computed at the end of the previous loading step. The confining pressure in the middle of each reinforced layer was obtained by multiplying the distributed vertical stress by the coefficient of lateral pressure (k_r). The value of k_r is proposed by authors as Eq. (29), in which the value of lateral pressure coefficient for unreinforced soil $k_{un}=0.5$ has been suggested by Madhavi Latha (2000). For the M=0, Eq. (29) results the lateral pressure coefficient of unreinforced soil (k_{un}).

$$k_r = k_{un} (K_u + 100 M^{0.1}) / K_u \tag{29}$$

Overall, Eqs. (25a) to (29) reveal that the proposed formulations would be able to consider the variation of geocell performance in regard to the strain level and confinement stress variations across the depth of the

329 foundation bed, provided the elastic modulus of the different layers (soil layers and the geocell-reinforced layers)

330 are allotted appropriate values that differ from layer-to-layer and from one loading step to the next. Based on the

331 results of triaxial compression tests, the value of the hyperbolic parameter of Duncan and Chang (1970), K_u, is

332 found as 483.3 (the authors' evaluation not reported here). Also, the secant modulus of the geocell material at

333 2.5% strain, M, is given by the manufacturer as 114 kN/m (M= 114 kN/m). Due to the confinement of the soil by

334 the geocell wall, the Poisson's ratio of geocell-reinforced layers may be less than that in unreinforced layers. The

335 range of Poisson's ratio for granular soil (i.e. sand in the present paper) is about 0.3-0.35 and for geocell filled

336 with sand from 0.17 (Mhaiskar and Mandal, 1996) to 0.25 (Zhang et al., 2010c). Thus, a Poisson's ratio of 0.3 is

337 used for unreinforced layers and a Poisson's ratio of 0.25, 0.2, and 0.2, is used respectively for reinforced layers

338 with one, two and three layers of geocell.

339 **8.2. Validation of proposed analytical method**

340   The presented analytical method was validated by comparing the results of model analyses with plate load

341 tests results (Moghaddas Tafreshi et al., 2013) for an unreinforced bed and for beds reinforced by one, two

342 and three layers of geocell. Fig. 10 compares the results of the analytical method and tests in the form of

343 footing pressure-settlement responses, for different values of geocell mass. These comparisons are done for

344 parameters of K_u=483.3, M= 114 kN/m, h_g=100 mm and D=300 mm. Since, the analytical method has not

345 considered any variation in the geocells' width; it is assumed that the width of the geocell-reinforced layers

346 being sufficient to ensure the anchorage derived from the adjacent stable soil mass.

347   The predicted responses show a better match with the experimental ones at lower footing settlement

348 levels (i.e., s/D<8%). For larger footing settlements (e.g., s/D>8%), the analytical predictions under-estimate

349 the experimentally determined settlements, implying strain softening in the geocell-soil layers in-situ relative

350 to the performance in the triaxial or that the assumption of no lateral strain is non-conservative. The

351 difference between the predicted responses and experimental ones might more generally be attributed to the

352 selected value of lateral pressure coefficient, the selected values of Poisson's ratio, the simplifying

353 assumptions used in the analytical method, the discrepancies between the experimental and analytical

354 systems and the differences in simulating the field and the experimental conditions of multiple layers.

355   Since the practical design of shallow footings is mostly governed by footing settlement, footing

356 settlement must be limited to specific values, depending on the super-structure. Thus, the close comparison of

357 analytical and experimental results in the lower range of settlement (i.e., less than 6% of the footing

358   diameter) is encouraging. This implies that the analytical method presented is capable of estimating the

359   behavior of footings supported by geocell layers and may be conveniently applied as a tool to estimate the

360   pressure-settlement response of footings over most practical ranges of geotechnical use.

361   **8.3. Predictive parametric study**

362   Using the analytical model presented, a parametric study was carried out to account for the variability of

363   those parameters that could not be considered in the physical tests, so as to verify the model's predictive

364   capability. Particularly, variation in the secant modulus of geocell (M), the dimensionless modulus number of the

365   soil (K_u), the thickness of geocell layers (h_g) and the number of geocell layers (N_g) were investigated in this way.

366   Fig. 11a shows the effect of the secant modulus of the geocell (M) on the pressure-settlement response of a

367   foundation reinforced with three layers of geocell. The results reveal the beneficial effect of the reinforcement's

368   rigidity (see Eq. (28)) in decreasing the footing settlements, so that at a given bearing pressure, the value of the

369   settlement decreases as the secant modulus of geocell (M) increases. The similar results reported by Madhavi

370   Latha et al. (2006) for geocell-supported embankments showed that higher surcharge capacity and lower

371   deformations are associated with increase in the value of the M parameter. This performance could be attributed

372   to the internal confinement provided by geocell reinforcement with increase in M. The confinement effect is

373   dependent on the secant modulus of the reinforcement, the friction at the soil-reinforcement interface and the

374   confining stress developed on the infilling soil inside the geocell pocket due to the passive resistance provided by

375   the 3D structure of geocell (Sireesh et al., 2009; Moghaddas Tafreshi and Dawson, 2010a). In addition, as seen in

376   Fig. 11a, there is a limiting value of M (=100 kN/m) beyond which no further load-settlement benefit is achieved.

377   Almost certainly this is because the behavior of the unreinforced soil between the reinforced layers is now

378   limiting the response of the overall system.

379   To see what the effect of K_u is, the variation of pressure-settlement of the reinforced bed with three layers

380   of geocell is presented in Fig. 11b. The results show that the bearing capacity of a footing at a given

381   settlement is significantly increased due to an increase in the K_u value. Thus, the role of the soil type and the

382   soil compaction in performance of geocell-reinforced beds, which the composite model suggested in the

383   present study, can take into account this effect. However, a dense sand matrix tends to dilate under footing

384   penetration, thereby mobilizing higher strength in the geocell reinforcement, leading to greater performance

385   improvement (Madhavi Latha et al., 2009b).

386   The rigidity of the geocell layer is predominantly influenced by the thickness of geocell. To have a better

387   assessment of the effect of a geocell's thickness in a geocell-reinforced foundation, the variation of the

388   pressure-settlement relationship of the unreinforced bed and of the reinforced bed with three layers of geocell

389   is presented in Fig. 11c. The benefit of a thicker geocell mat is evident, so that a thicker geocell decreases the

390   footing settlements, tending to improve its bearing capacity. This appears to be a consequence of greater

391   opportunity of geocell-soil interaction (in the form of wall-friction and confining pressure imposed by the

392   pocket walls) and the increased stiffness of the effective zone beneath the footing consequent upon an

393   increase in the thickness of geocell. This is in-line with the findings of Dash et al. (2007), Sitharam et al.

394   (2007), Madhavi Latha et al. (2006) Moghaddas Tafreshi and Dawson (2010a) who reported that the

395   settlement of a trench's soil surface was decreased due to the provision of a thicker geocell in the backfill.

396   Furthermore, the rate of reduction in footing settlement and the rate of enhancement in load carrying capacity

397   of the footing can also be seen to reduce with increase in the value of h_g. The reason is that, as multiple,

398   thicker reinforcement layers are used, then the reinforced zone extends deeper beyond the zone most

399   significantly strained by the applied load, so that little further benefit accrues. From a practical point of view,

400   as the thickness of a geocell layer is increased; the problem of lower achieved compaction in the geocell

401   packets would be encountered, so that higher compactive effort is necessary as the thickness of vertical webs

402   of the geocell is increased, owing to hindering of vertical densification (Thakur et al., 2012; Tavakoli

403   Mehrjardi et al., 2013). For this reason, multiple thin geocell layers may, in practice, be preferred to fewer,

404   thicker layers.

405   Fig. 11d presents the bearing pressure-settlement response of the unreinforced and reinforced foundation

406   beds with one, two, three layers of geocell. From this figure, it may be clearly observed that, as the number of

407   geocell layers increases (i.e., the increase in the depth of the reinforced zone), both stiffness and bearing

408   pressure at a specified settlement increase substantially. Likewise, at a given bearing pressure, the value of

409   the settlement decreases as the number of geocell layers increases. However, the rate of reduction in footing

410   settlement is seen to reduce with increase in the number of geocell layers. It is likely that the additional layers

411   are interacting with soil that is strained less and less by the applied load, therefore delivering diminishing

412   increments of additional reinforcement effect. Yoon et al. (2008) and Moghaddas Tafreshi et al. (2013) in

413   their studies on the effect of multi-layered geocell reported a similar effect with increase in the number of 3D

414   reinforcement layers.

415   **9. Conclusions**

In this study, an analytical approach based on the theory of multi-layered soil system theory (Hirai, 2008; Vakili et al., 2008) was developed to estimate the pressure-settlement response of a circular footing supported by unreinforced and multi-layered reinforced beds. Definition of elastic modulus for unreinforced and reinforced layers in terms of strain and confining pressure, along with the equivalent elastic method were the main processes of problem solution. The new method delivers predictions of load-settlement that are in good agreement with measured values for a geocell-reinforced application, and thus gives confidence of its usefulness for expected geotechnical applications. The results of the new model, as applied to geocell installations, can be summarized as follows:

(1) The response of pressure-settlement in both reinforced and unreinforced conditions is nonlinearly and significantly affected by the secant modulus of geocell, the dimensionless modulus number of the soil, thickness of geocell layers and the number of geocell layers.

(2) The results emphasized that the performance of geocell-reinforced foundation is always much better than when unreinforced.

(3) The analytical results show that the increase in the number of geocell layers, the secant modulus of the geocell and the dimensionless modulus number of the soil, strengthen the behavior of geocell-reinforced foundation against the surface loading, which is in-line with the experimental results of researchers.

(4) The parametric study shows a decrease in rate of enhancement in bearing pressure, at a given footing settlement with increase in the number of geocell layers, the secant modulus and the thickness of geocell layers.

It should be stated that the results obtained are based on a circular loading plate, one type of geocell reinforcement, fixed width of geocell layers and non-cohesive soil. Consequently, specific applications should only be made after considering the above limitations.

References

American Society for Testing and Materials, 2011. Standard practice for classification of soils for engineering purposes (Unified Soil Classification System). ASTM International, West Conshohocken, PA, D 2487-11.

Avesani Neto, J.O., Bueno, B.S., Futai, M.M., 2013. A bearing capacity calculation method for soil reinforced with a geocell. Geosynth. Int. 20 (3), 129 –142.

443   Bathurst, R.J., Nernheim, A., Walters, D.L., Allen, T.M., Burgess, P., Saunders, D.D., 2009. Influence of reinforcement

444   stiffness and compaction on the performance of four geosynthetic – reinforced soil walls. Geosynth. Int. 16 (1), 43–

445   49.

446   Biswas, A., .Murali Krishna, A., Dash, S.K., 2013. Influence of subgrade strength on the performance of geocell-

447   reinforced foundation systems. Geosynth. Int. 20 (6), 376 –388.

448   Boushehrian, A.H., Hataf, N., Ghahramani, A., 2011. Modeling of the cyclic behavior of shallow foundations resting on

449   geomesh and grid-anchor reinforced sand. Geotext. Geomembr. 29 (3), 242-248.

450   Chen, R.H., Chiu, Y.M., 2008. Model tests of geocell retaining structures. Geotext. Geomembr. 26 (1), 56-70.

451   Chen, R.H., Huang, Y.W., Huang, F.C., 2013. Confinement effect of geocells on sand samples under triaxial

452   compression. Geotext. Geomembr. 37 (2), 35-44.

453   Chen, R.H., Wu, C.P., Huang, F.C., Shen, C.W., 2013. Numerical analysis of geocell-reinforced retaining structures.

454   Geotext. Geomembr. 39 (4), 51-62.

455   Collin, J.G., Kinney, T.C., Fu, X., 1996. Full scale highway load test of flexible pavement systems with geogrid

456   reinforced base courses. Geosynth. Int. 3 (4), 537–549.

457   Dash, S.K., Rajagopal, K., Krishnaswamy, N.R., 2007. Behaviour of geocell reinforced sand beds under strip loading.

458   Can. Geotech. J. 44 (7), 905–916.

459   Dash, S.K., Chandra Bora, M., 2013. Improved performance of soft clay foundations using stone columns and geocell-

460   sand mattress. Geotext. Geomembr. 41 (November), 26-35.

461   Duncan, J. M., Chang, C. Y., 1970. Nonlinear analysis of stress and strain in soils. J. Soil Mech. and Found. 96 (5),

462   1629–1653.

463   Foster, C. R., Ahlvin, R. G., 1959. Stresses and deflections induced by a uniform circular load, Proc. Highway Research

464   Board. 33, 467-470.

465   Harr, M.E., 1966. Foundations of theoretical soil mechanics. McGraw-Hill: New York.

466   Hegde, A., Sitharam, T.G., 2015. 3-Dimensional numerical modelling of geocell reinforced sand beds. Geotext,

467   Geomembr. 43 (2), 171–181.

468   Hegde, A., Sitharam, T.G., 2015. 3-Dimensional numerical analysis of geocell reinforced soft clay beds by considering
469   the actual geometry of geocell pockets. Can. Geotech. J. Published on the web 14 February 2015, 10.1139/cgj-2014-
470   0387.

471   Hirai, H., Kamei, T.A., 2003. A method to calculate settlement, stress and allowable stress of multi-layered ground. J.of
472   Struct. Constr. Eng. 573, 81–88.

473   Hirai, H., Kamei, T., 2004. A method to calculate settlement, stress, failure and allowable stress of multi-layered ground
474   by equivalent thickness theory. J. of Struct. Constr. Eng. 581, 79–86.

475   Hirai, H., 2008. Settlements and stresses of multi-layered grounds and improved grounds by equivalent elastic method.
476   International. J. for Num. Analy. Meth. Geomech. 32 (5), 523–557.

477   Eid, H.T., Alansari, O.A., Odeh, A.M., Nasr, M.N., Sadek, H.A., 2009. Comparative study on the behavior of square
478   foundations resting on confined sand. Can. Geotech. J. 46 (4), 438-453.

479   Huang, C.C., 2014. Force equilibrium-based finite displacement analyses for reinforced slopes: Formulation and
480   verification. Geotext. Geomembr. 42 (4), 394-404.

481   Hufenus, R., Rueegger, R., Banjac, R., Mayor, P., Springman, S.M., Bronnimann, R., 2006. Full-scale field tests on
482   geosynthetic reinforced unpaved on soft subgrade. Geotext. Geomembr. 24 (1), 21–37.

483   Indraratna, B., Biabani, M., Nimbalkar, S., 2015. Behavior of Geocell-Reinforced Subballast Subjected to Cyclic Loading
484   in Plane-Strain Condition. J. Geotech. Geoenviron. Eng. 141 (1), 10.1061/ (ASCE) GT.1943-5606.0001199.

485   Kachi, T.,Kobayashi, M., Seki, M., Koseki, J., 2013. Reinforcement of railway ballasted track with geosynthetic bags for
486   preventing derailment. Geosynth. Int. 20 (5), 316 –331.

487   Kumar, A., Kaur, A., 2012. Model tests of square footing resting on fibre-reinforced sand bed. Geosynth. Int. 19 (5), 385-
488   392.

489   Lambert, S., Nicot, F.,Gotteland, P., 2011. Uniaxial compressive behavior of scrapped tire and sand-filled wire netted
490   geocell with a geotextile envelope. Geotext, Geomembr. 29 (5), 483-490.

491   Leshchinsky, B., Ling, H., 2013a. Numerical modeling of behavior of railway ballasted structure with geocell
492   confinement. Geotext. Geomembr. 36 (1), 33–43.

493   Leshchinsky, B., Ling, H., 2013b. Effects of Geocell Confinement on Strength and Deformation Behavior of Gravel. J.
494   Geotech. Geoenviron. Eng. 139 (2), 340-352.

495   Ling, H., Leshchinsky, D., Wang, J.P., Mohri, Y., Rosen, A., 2009. Seismic Response of Geocell Retaining Walls:
496   Experimental Studies. J. Geotech. Geoenviron. Eng. 135 (4), 515-524.

497   Madhavi Latha, G.M., 2000. Investigation on the behavior of geocell supported embankments. Ph.D. Thesis, Department
498   of Civil Engineering, Indian Institue of Technology Madras, Chennai.

499   Madhavi Latha, G.M., Rajagopal, K., Krishnaswamy, N. R., 2006. Experimental and theoretical investigations on
500   geocell-supported embankments. Int. J. of Geomech. ASCE, 6 (1), 30–35.

501   Madhavi Latha, G.M., Rajagopal, K. 2007. Parametric finite element analyses of geocell supported embankments. Can.
502   Geotech. J. 44 (8), 917-927.

503   Madhavi Latha, G.M., Somwanshi, A., 2009a. Bearing capacity of square footings on geosynthetic reinforced sand.
504   Geotext. Geomembr. 27 (4), 281–294.

505   Madhavi Latha, G.M., Dash, S. K., Rajagopal, K., 2009b. Numerical simulation of the behavior of geocell reinforced. Int.
506   J. of Geomech. ASCE, 9 (4), 143–152.

507   Mehdipour, I., Ghazavi, M., Ziaie Moayed, R., 2013. Numerical study on stability analysis of geocell reinforced slopes
508   by considering the bending effect. Geotext. Geomembr. 37 (April), 23-34.

509   Mhaiskar, S.Y., Mandal, J.N., 1996. Investigations on soft clay subgrade strengthening using geocells. Construc. Build.
510   Mater. 10 (4), 281–286.

511   Moghaddas Tafreshi, S.N., Dawson, A.R., 2010a. Comparison of bearing capacity of a strip footing on sand with geocell
512   and with planar forms of geotextile reinforcement. Geotext. Geomembr. 28 (1), 72–84.

513   Moghaddas Tafreshi, S.N., Dawson, A.R. 2010b. Behaviour of footings on reinforced sand subjected to repeated loading
514   – Comparing use of 3D and planar geotextile. Geotext. Geomembr. 28 (5), 434–447.

515   Moghaddas Tafreshi, S.N., Khalaj, O., Dawson, A.R., 2013. Pilot-scale load tests of a combined multi-layered geocell
516   and rubber-reinforced foundation. Geosynth. Int. 20 (3), 143–161.

517   Moghaddas Tafreshi, S.N., Khalaj, O., Dawson, A.R., 2014. Repeated loading of soil containing granulated rubber and
518   multiple geocell layers. Geotext. Geomembr. 42 (1), 25-38.

519   Noori, B., 2012. Experimental investigation of the behavior of geocell reinforced rubber-soil mixture, Msc thesis, Faculty
520   of Civil Engineering, K.N. Toosi University of Technology, Tehran, Iran.

521   Odemark, N., 1949. Investigations as to the elastic properties of soils and design of pavements according to the theory of

522   elasticity. Statens Vaginstitute: Meddelande, Stockholm, Sweden, vol. 77.

523   Palmeira, E.M., Andrade, H.K.P.A., 2010. Protection of buried pipes against accidental damage using geosynthetics.

524   Geosynth. Int. 17 (4), 228–241.

525   Palmer, L.A., Barber, E.S., 1940. Soil displacement under a circular loaded area. Proceedings of the Highway Research

526   Board, 20, 279–286.

527   Pokharel, S. K., Han, J., Leshchinsky, D., Parsons, R. L., Halahmi, I., 2010. Investigation of factors influencing behavior

528   of single geocell-reinforced bases under static loading. Geotext. Geomembr. 28 (6), 570-578.

529   Pokharel, S. K., 2010. Experimental Study on Geocell-Reinforced Bases under Static and Dynamic Loading, PhD thesis,

530   Univ. Kansas, USA.

531   Raymond, G.P., 2002. Reinforced ballast behaviour subjected to repeated load. Geotext. Geomembr. 20 (9), 39-61.

532   Sharma, R., Chen, Q., Abu-Farsakh, M., Yoon, S., 2009. Analytical modeling of geogrid reinforced soil foundation.

533   Geotext. Geomembr. 27 (1), 63–72.

534   Sireesh, S., Sitharam, T.G., Dash, S.K., 2009. Bearing capacity of circular footing on geocell–sand mattress overlying

535   clay bed with void. Geotext. Geomembr. 27 (2), 89–98.

536   Sitharam, T.G., Sireesh, S., Dash, S.K., 2007. Performance of surface footing on geocell-reinforced soft clay beds.

537   Geotech. Geolo. Eng. 25 (5), 509–524.

538   Song, F., Xie, Y.L., Yang, Y.F., Yang, X.H., 2014. Analysis of failure of flexible geocell-reinforced retaining walls. in

539   the centrifuge. Geosynth. Int. 21(6,) 342 –351.

540   Soudé, M., Chevalier, B., Grédiac, M., Talon, A., Gourvès, R., 2013. Experimental and numerical investigation of the

541   response of geocell-reinforced walls to horizontal localized impact. Geotext. Geomembr. 39 (August), 39-50.

542   Tanyu, B.F., Aydilek, A.H., Lau, A.W., Edil, T.B., Benson, C.H. 2013. Laboratory evaluation of geocell-reinforced

543   gravel subbase over poor subgrades. Geosynth. Int. 20 (2), 47 –61.

544   Tavakoli Mehrjardi, Gh., Moghaddas Tafreshi, S.N., Dawson, A.R., 2012. Combined use of geocell reinforcement and

545   rubber–soil mixtures to improve performance of buried pipes. Geotext. Geomembr. 34 (October), 116-130.

546   Tavakoli Mehrjardi, Gh., Moghaddas Tafreshi, S. N., Dawson, A. R., 2013. Pipe response in a geocell reinforced trench

547   and compaction considerations. Geosynth. Int. 20 (2), 105-118.

548   Terzaghi K. Theoretical Soil Mechanics. Wiley: New York, 1943.

549   Thakur, J.K., Han, J., Pokharel, S.K., Parsons, R.L., 2012. Performance of geocell-reinforced recycled asphalt pavement

550   (RAP) bases over weak subgrade under cyclic plate loading. Geotext. Geomembr. 35 (December), 14-24.

551   Yang, X., Han, J., Pokharel, S.K., Manandhar, C., Parsons, R.L., Leshchinsky, D., Halahmi, I., 2012. Accelerated

552   pavement testing of unpaved roads with geocell-reinforced sand bases. Geotext. Geomembr. 32, (June), 95-103.

553   Yang, X., Han, J., 2013. Analytical Model for Resilient Modulus and Permanent Deformation of Geosynthetic-

554   Reinforced Unbound Granular Material. . J. Geotech. Geoenviron. Eng. 139 (9), 1443-1453.

555   Yoon, Y. W., Heo, S. B., Kim, S. K., 2008. Geotechnical performance of waste tires for soil reinforcement from chamber

556   tests. Geotext. Geomembr. 26 (1), 100-107.

557   Vakili Ninyo, J., Moore, I., 2008. A simplified method for evaluation of pavement layers moduli using surface deflection

558   data. The 12th International Conference of International Association for Computer Methods and Advances in

559   Geomechanics (IACMAG), Goa India, 1-6.

560   Wesselo, J., Visser, A.T., Rust, E., 2009. The stress–strain behaviour of multiple cell geocell packs. Geotext. Geomembr.

561   27 (1), 31-38.

562   Wu, J.T.H., Pham, T.Q. Adams, M.T., 2013. Composite Behavior of Geosynthetic Reinforced Soil Mass. Denver, Co.,

563   University of Colorado Denver, Dept. of Civil Engineering ; McLean, VA : Federal Highway Administration, Office

564   of Infrastructure Research and Development, 2013-07 (FHWA-HRT-10-077), 214 pp.

565   Zhang, L., Zhao, M., Zou, X., Zhao, H. 2009. Deformation analysis of geocell reinforcement using Winkler model.

566   Comput. Geotech. 36 (6), 977-983.

567   Zhang, L., Zhao, M., Shi, C., Zhao, H., 2010a. Bearing capacity of geocell reinforcement in embankment engineering.

568   Geotext. and Geomembr. 28(5), 475-482.

569   Zhang, L., Zhao, M., Zou, X., Zhao, H. 2010b. Analysis of geocell-reinforced mattress with consideration of horizontal–

570   vertical coupling. Comput. Geotech. 37 (6), 748–756.

571   Zhang, L., Qiangkang, Gu., Guoping, Cen., 2010c. Effect of Geo-Cell Reinforced Soil Structure Used in Flexible Airfield

572   Pavement. iclem logistics for sustained economic development, ASCE. 1629-1635.

573   Zhou, H.B., Wen, X.J., 2008. Model studies on geogrid- or geocell-reinforced sand mattress on soft soil. Geotext.

574   Geomembr. 26(3), 231–238.

575 **Nomenclature**

a	Loading plate radius *(m)*
b	Width of the geocell layers *(m)*
a_1, a_2, b_1 and b_2	Model parameters to estimate the elastic modulus of gocell-reinforced layers
D	Loading plate diameter *(m)*
D_f	Embedment depth of footing *(m)*
E_g	Elastic modulus of layer of geocell and soil *(kPa)*
E_H	Equivalent elastic modulus of upper soil layer of thickness H *(kPa)*
E_i, E_j, E_m, E_n	Elastic modulus of layer i, j, m, n *(kPa)*
$f(\varepsilon)$	Function to consider the strain level in estimating the elastic modulus of unreinforced and geocell-reinforced layers
H_e	Equivalent thickness *(m)*
H_{1e}	Equivalent thickness of the first layer *(m)*
H_{me}	Equivalent thickness of the mth layer *(m)*
H_{eff}	Effective depth *(m)*
H_{ie}	Equivalent thickness of the each layer *(m)*
h_g	Height of geocell layers *(m)*
H_m	Thickness of mth layer *(m)*
h_s	Vertical spacing of the geocell layers *(m)*
k_r	Lateral pressure coefficient for geocell-reinforced layers
K_u	Dimensionless modulus number of the unreinforced sand in the hyperbolic model
k_{un}	Lateral pressure coefficient for unreinforced layers
M	Secant tensile modulus of the geocell material at an average strain of 2.5% *(kN/m)*
MLE	Multiple Linear Elastic
n	Number of layers of multilayered system
N_g	Number of geocell layers
u	Vertical distance of the first layer of geocell from the footing *(m)*

q	Uniform pressure on a circular footing with radius "a" *(kPa)*
w	Actual total surface settlement at the center of the circular loading surface *(m)*
w^j	Vertical displacement at surface of system for loading of q_j *(m)*
w_0	Vertical deflection at the center of loading on surface (at depth of $z=0$) of uniform equivalent layer *(m)*
w_1	Vertical deflection at bottom of the equivalent layer *(m)*
w_i	Vertical deflection on top of ith equivalent layer *(m)*
w_{pi}	Vertical thinning of ith original layer with thickness of H_i *(m)*
w_2	Vertical thinning of the original layer with thickness of H *(m)*
z	Depth of the backfill *(m)*
Δw	Vertical deformation (thinning) increment *(m)*
Δw_i^j	Displacement increment of equivalent layer for i^{th} layer *(m)*
$(\Delta w_p)_i^j$	Deformation increment (thinning) of layer with thickness of H_i for loading increment $q_j - q_{j-1}$ *(m)*
Δw_1^j	Vertical displacement increment on loading centerline at a depth of H_e for loading increment of $q_j - q_{j-1}$ *(m)*
Δw_0^j	Vertical displacement increment at surface (of equivalent layer) beneath centre of load for loading increment of $q_j - q_{j-1}$ *(m)*
Δw_2^j	Vertical deformation (thinning) increment of the original layer of thickness of H *(m)*
ε_i	Strain across the thickness of the ith layer *(%)*
ε_i^j	Strain of layer with thickness of H_i subjected to loading q_j *(%)*
φ	Angle of shearing resistance of soil being reinforced *(degree)*
v_n	Poisson's ratio of layer n
σ_d	Deviatoric stress *(kPa)*
σ_1	Vertical stress *(kPa)*
σ_3	Confining pressure *(kPa)*

576
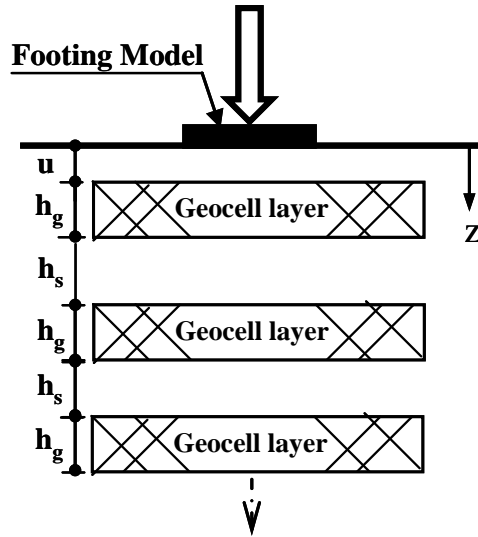
Fig. 1. Schematic of multi-layered geocell-reinforced foundation bed

577

578

579

580
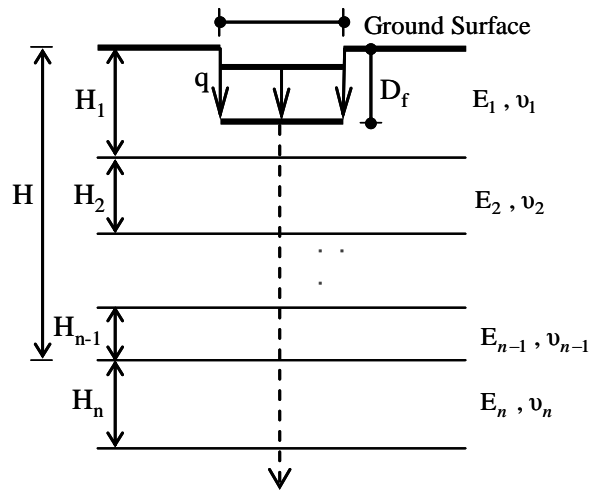
Fig. 2. Multi-layered soil systems (Hirai, 2008)

581

582

583

584
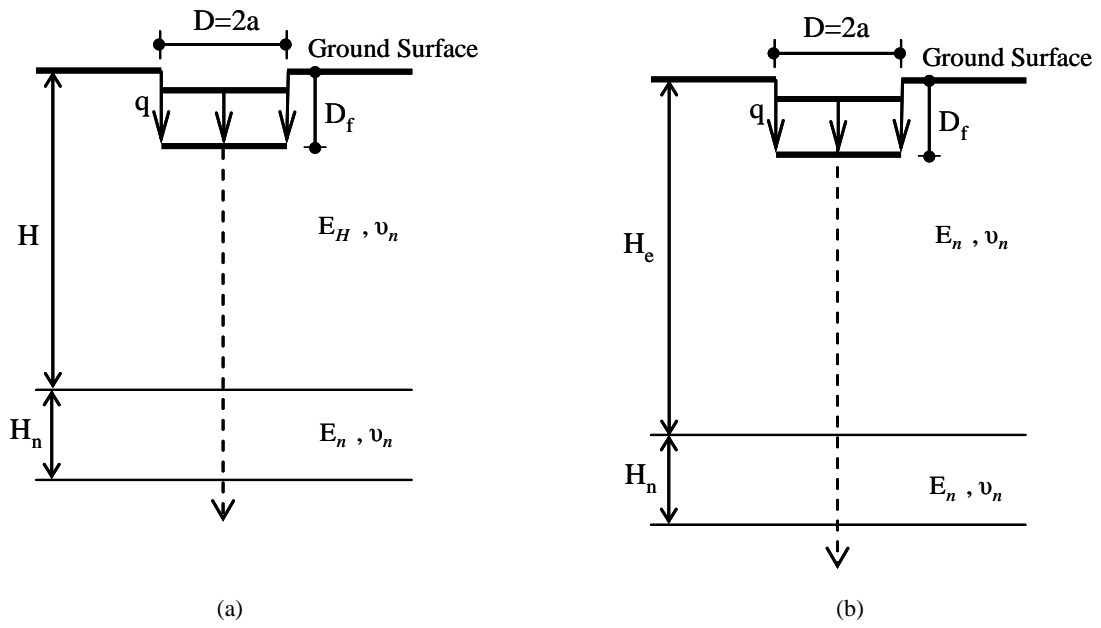
Fig. 3. (a) Equivalent two-layered soil system for Fig. 2 (b) Equivalent single layer soil system with the same E_n and v_n for

Fig. 3a. (Hirai, 2008)
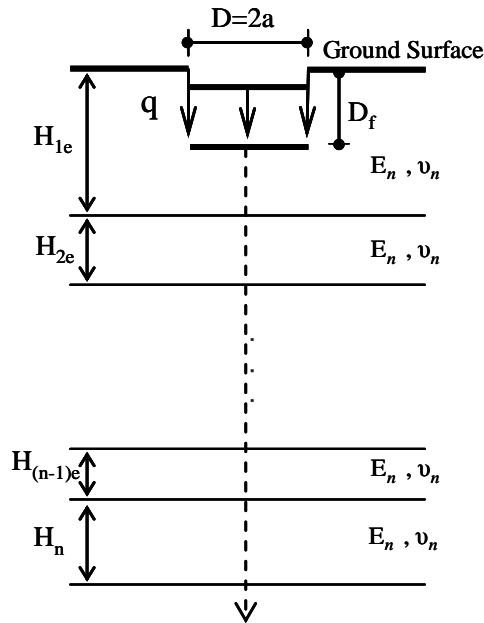
Fig. 4. Equivalent single soil layer with equivalent thickness of "$H_{1e}+H_{2e}+H_{3e}+\ldots+H_{(n-1)e}+H_n$"
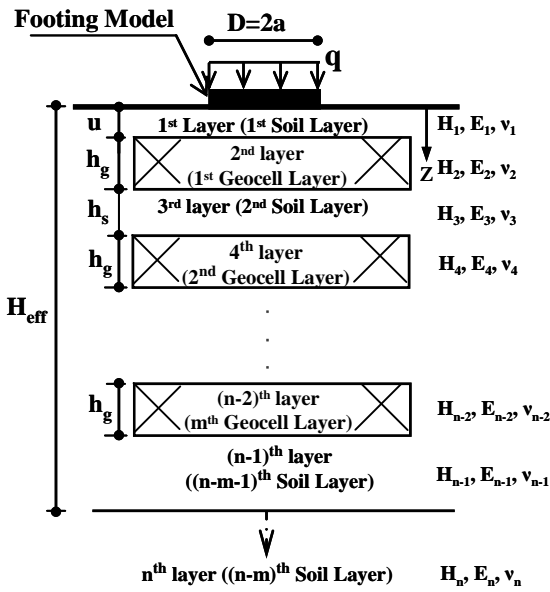
and E_n and v_n for Fig. 2 (Hirai, 2008)

588

589

Fig. 5. "n" layer geocell-reinforced soil system containing "m" layers of geocell.

597
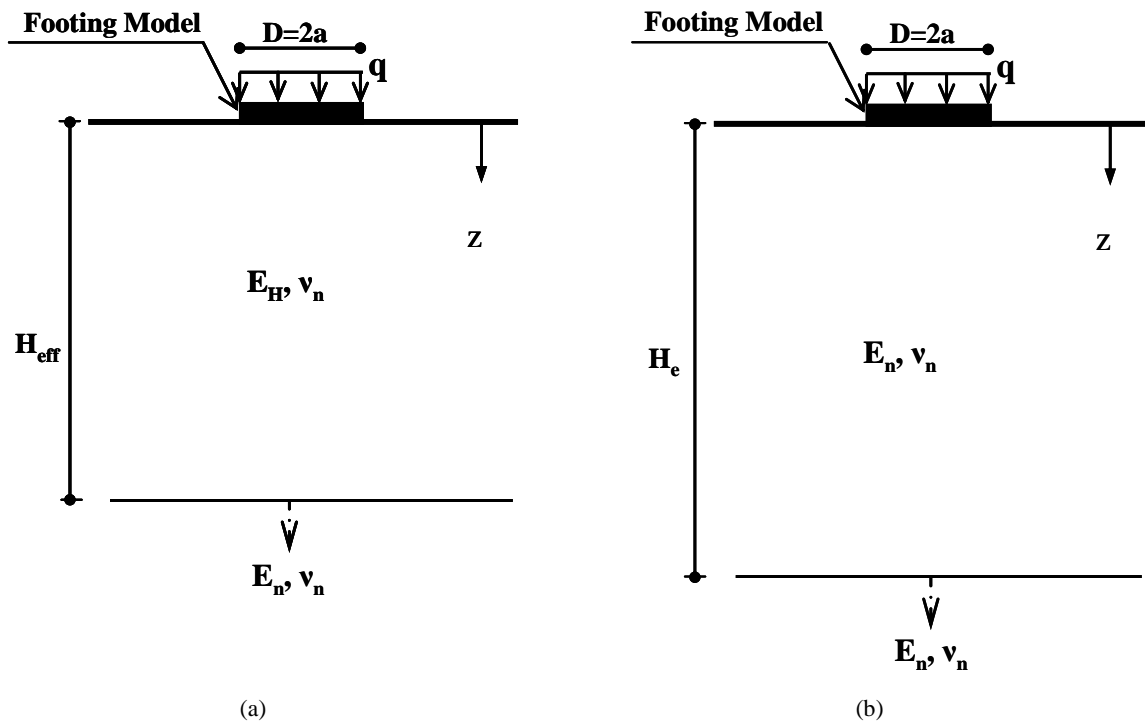
Fig. 6. Substituting n-layer system sequentially with (a) Equivalent two-layered system for n-layer system in Fig. 5 (b) Equivalent single layer system with the same E_n and ν_n for two-layered system in Fig. 6a.

598
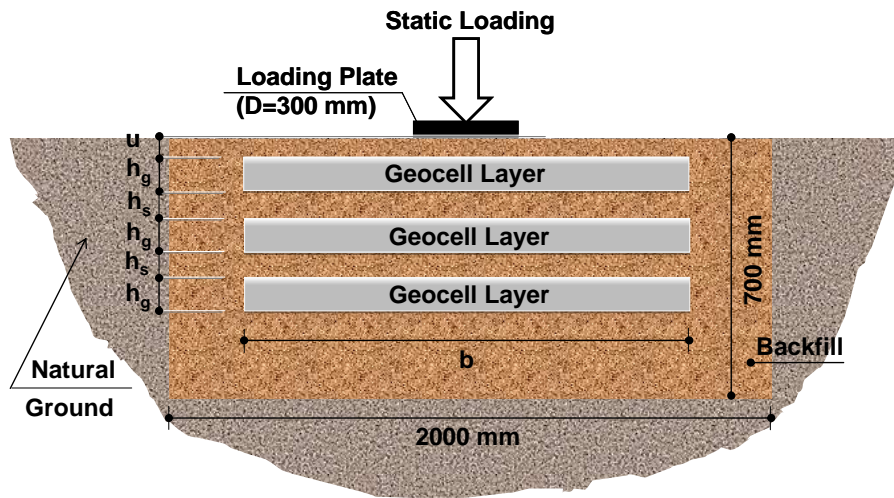
Fig. 7. Geometry of the test configurations used to validate the results of the method presented (*D*=300 mm, *u*=*h_s*=0.2*D*=60 mm, *h_g*=100 mm and *b/D*=5 (Moghaddas Tafreshi et al., 2013)).

599

(a)   (b)
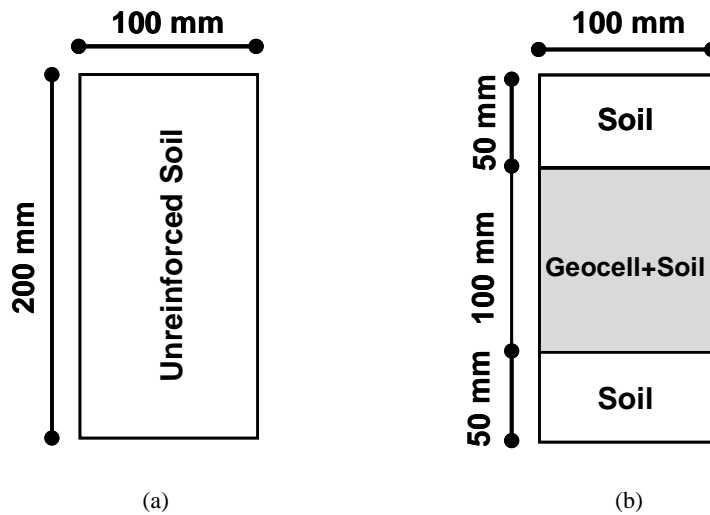
Fig. 8. Configurations used in triaxial tests (a) unreinforced (b) reinforced with one layer of geocell (Noori, 2012).

600

601

602
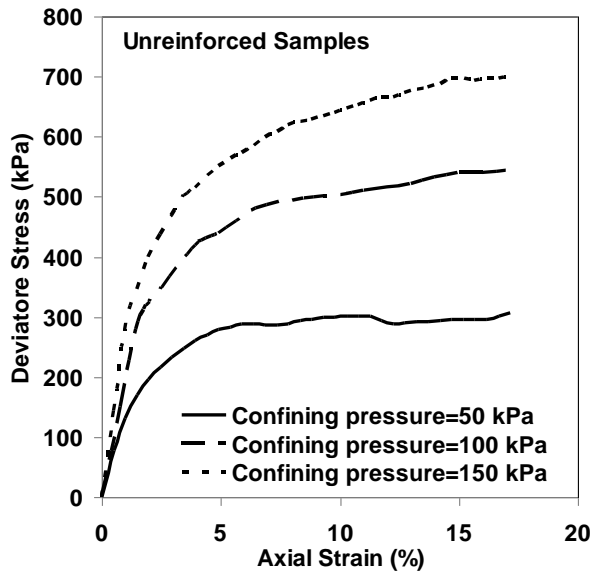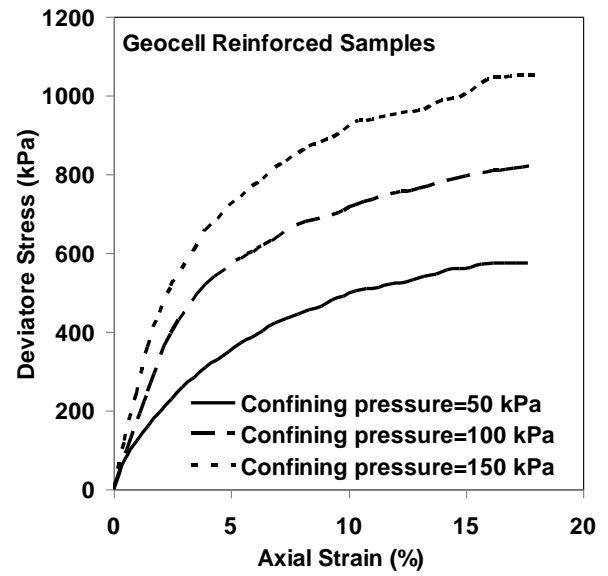
Fig. 9. Stress-axial strain curves for unreinforced and geocell reinforced samples under confining pressure of 50, 100 and 150 kPa (a) unreinforced samples, (b) geocell reinforced samples (Noori, 2012).

603
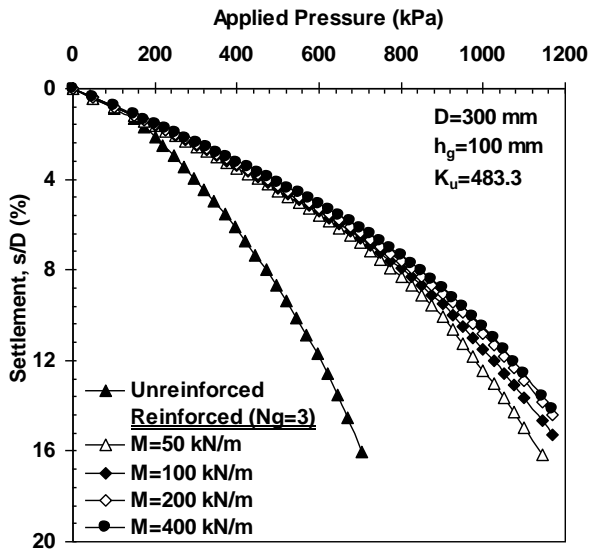
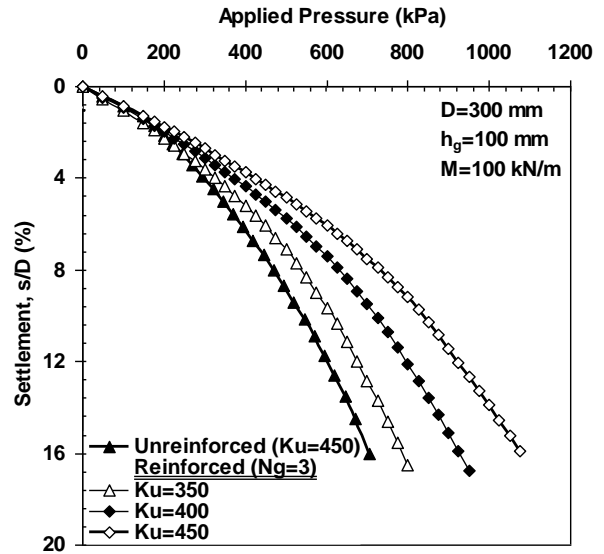604

605

606

607

608

609

610

611

612

613

614

615
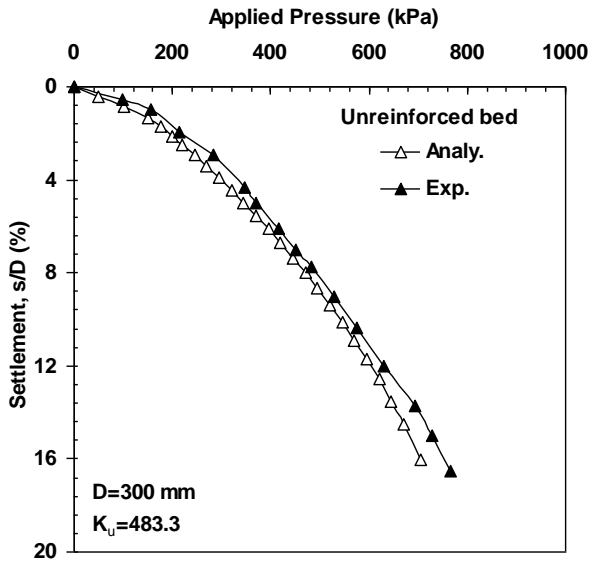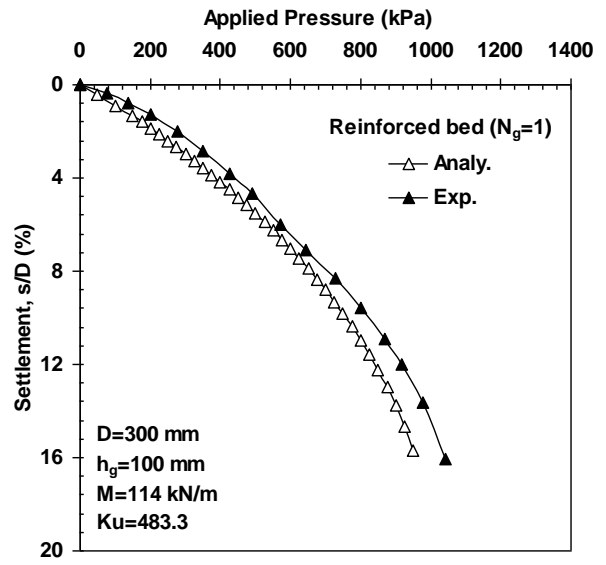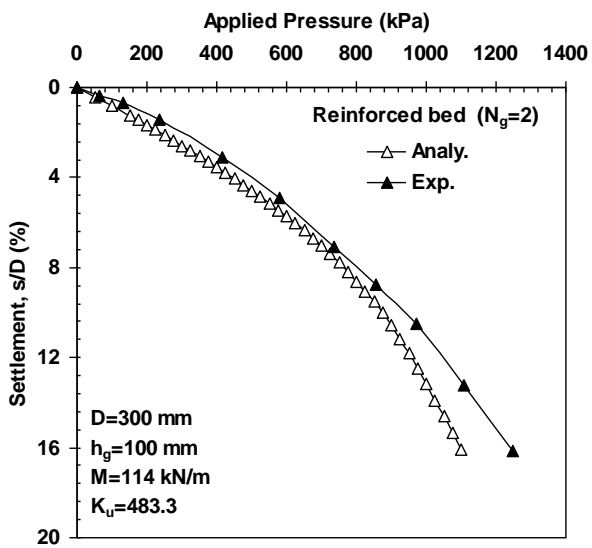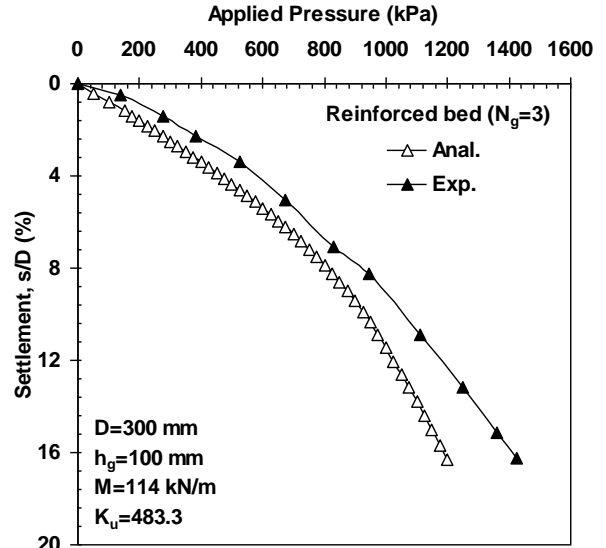
Fig. 10. Comparison of analytical and experimental results for (a) unreinforced bed, (b) reinforced bed with one layer of geocell, (c) reinforced bed with two layers of geocell, (d) reinforced bed with three layers of geocell
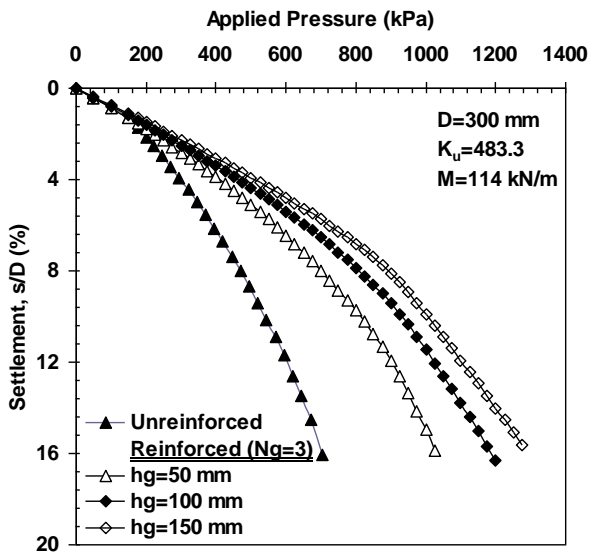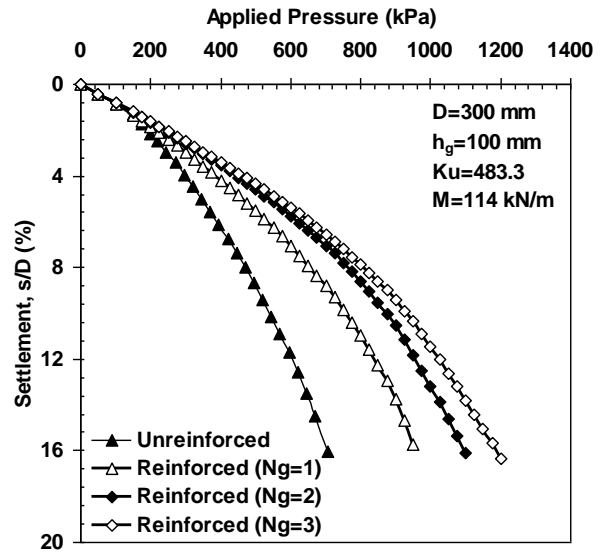
617

Fig. 11. Variation of pressure-settlement response of geocell-reinforced bed for different (a) secant modulus of geocell (*M*), (b) soil dimensionless modulus (K_u), (c) thickness of geocell layers (h_g), and (d) number of geocell layers (N_g)

618

619

620

621

622